2142 *Inorg. Chem.* **1984**, *23*, 2142-2148

Contribution from the Anorganisch Chemisch Laboratorium and Laboratorium voor Kristallografie,
University of Amsterdam, Nieuwe Achtergracht 166, 1018 WV Amsterdam, The Netherlands

Ruthenium Carbonyl 1,4-Diaza-1,3-butadiene (R-DAB) Complexes. 5.[1] Syntheses, Spectroscopic Properties, and Reactivity of $Ru_2(CO)_5$(alkyl-DAB), a Key Intermediate in the $Ru_3(CO)_{12}$–alkyl-DAB Reaction. Crystal and Molecular Structure of (1,4-Diisopropyl-1,4-diaza-1,3-butadiene)pentacarbonyldiruthenium, $Ru_2(CO)_5$(*i*-Pr-DAB)

JAN KEIJSPER,† LOUIS POLM,† GERARD VAN KOTEN,† KEES VRIEZE,*† GERT ABBEL,‡
and CASPER H. STAM‡

Received August 3, 1983

Removal of a CO group from $Ru_2(CO)_6$(R-DAB) (**1**) (R-DAB = 1,4-disubstituted 1,4-diaza-1,3-butadiene, RN=C(H)C(H)=NR), by heating or by treatment with Me_3NO, results in the formation of a very reactive species $Ru_2(CO)_5$(R-DAB) (**2**) (R = *i*-Pr, c-Hx, *t*-Bu). During this reaction the coordination of the R-DAB ligand changes from the 6e (σ-N, μ^2-N′, η^2-C=N′) to the 8e (σ-N, σ-N′, η^2-C=N, η^2-C′=N′) mode, which was demonstrated by an X-ray structure determination of $Ru_2(CO)_5$(*i*-Pr-DAB). Crystals of $Ru_2(CO)_5$(*i*-Pr-DAB) are orthorhombic with space group $P2_12_12_1$, cell constants a = 12.775 (2) Å, b = 13.518 (3) Å, and c = 9.636 (10) Å, and Z = 4. In the refinement, 1480 reflections were used, which results in a final R value of 0.045. The single Ru(1)–Ru(2) bond (2.741 (1) Å) is spanned by an asymmetric bridging carbonyl group with Ru(1)–C(3) (2.15 (1) Å) significantly longer than Ru(2)–C(3) (2.03 (1) Å), while the C(3)–O(3) vector is almost perpendicular (87°) to the Ru(1)–Ru(2) vector. The Ru–CO(terminal) bond lengths are equal, i.e. 1.86 (1) Å (mean). The *i*-Pr-DAB ligand has a flat N=CC=N skeleton and is chelate bonded to Ru(2) with two equal bond lengths (2.14 (1) Å) and η^2-C=N,η^2-C′=N′ bonded to Ru(1) with four equal bond lengths (2.27 (1) Å). The complexes have been further characterized by ^1H NMR, IR, and FD mass spectroscopy. These techniques indicated similar geometries in solution and in the solid state. $Ru_2(CO)_5$(R-DAB) (**2**) reacts easily with CO, yielding $Ru_2(CO)_6$(R-DAB) (**1**) (R = *i*-Pr, c-Hx, *t*-Bu), and with R-DAB, yielding $Ru_2(CO)_5$(R-IAE) (**3**) (R = *i*-Pr, c-Hx, *t*-Bu; R-IAE = bis[(R-imino)(R-amino)ethane]) and $Ru_2(CO)_4$(*neo*-Pe-DAB)$_2$ (**3′**). Thermal decomposition of $Ru_2(CO)_5$(R-DAB) yielded the known compound $Ru_4(CO)_8$(R-DAB)$_2$ (**4**) (R = *i*-Pr, c-Hx, *neo*-Pe). Reaction with $Fe_2(CO)_9$ and $Ru_3(CO)_{12}$ yielded the novel complexes $FeRu(CO)_6$(R-DAB) (**5**) (R = *i*-Pr, c-Hx, *t*-Bu) and $Ru_3(CO)_8$(R-DAB) (**6**) (R = *neo*-Pe, *i*-Bu), which were characterized by FD mass, IR, and NMR spectroscopy. These reactions prove that $Ru_2(CO)_5$(R-DAB) is a key intermediate in the $Ru_3(CO)_{12}$–R-DAB reaction sequence as well as in the earlier developed reactions of $Ru_2(CO)_6$(R-DAB) with unsaturated molecules.

Introduction

1,4-Disubstituted 1,4-diaza-1,3-butadienes (R-DAB) react with metal carbonyls leading to complexes with the R-DAB ligand bonded in a wide variety of coordination modes.[2] Especially from the reaction of R-DAB with $Ru_3(CO)_{12}$ a great number of novel Ru–carbonyl–R-DAB products have been isolated, ranging from mononuclear $Ru(CO)_3$(R-DAB) to di-, tri-, and tetranuclear species.[3] Some of these products show a rich chemistry, due to the fact that they contain a R-DAB ligand of which one C=N bond is activated. For example, $Ru_2(CO)_6$(R-DAB), in which a 6e(σ-N, μ^2-N′, η^2C=N′) coordination of the R-DAB ligand is present, reacts with different kinds of unsaturated molecules such as α-diimines,[4] acetylenes,[5] diimides, and sulfines,[6a] leading to complexes with R-DAB linked to the new ligand via a C–C bond. This type of C–C coupling reaction, which has also been found by Knox et al.[7b–d] on Ru_2 centers, linking e.g. CO and alkynes or olefins and methylcarbynes, is shown schematically in Figure 1.

However, although further studies revealed the way in which the steric properties of R influenced the type of Ru–carbonyl–R-DAB product,[3] the reaction pathways leading to these different products remained unclear. As a possible sequence for the reaction of $Ru_3(CO)_{12}$ with R-DAB, a substitution of two CO groups, yielding $Ru_3(CO)_{10}$(R-DAB), was proposed as a first step followed by the formation of $Ru(CO)_3$(R-DAB), $Ru_2(CO)_6$(R-DAB), or $Ru_3(CO)_8$(R-DAB), depending on R.[3,8,9] However, on the basis of present results,

---

† Anorganisch Chemisch Laboratorium.

‡ Laboratorium voor Kristallografie.

(1) For earlier parts, see ref 3–5 and 13.

(2) (a) Fruehauf, H. W.; Landers, A.; Goddard, R.; Krueger, C. *Angew. Chem.* **1978**, *90*, 56. (b) van Koten, G.; Vrieze, K. *Recl. Trav. Chim. Pays-Bas* **1981**, *100*, 129. (c) Kokkes, M. W.; Stufkens, D. J.; Oskam, A. *J. Chem. Soc., Dalton Trans.* **1983**, 439. (d) Bock, H.; tom Dieck, H. *Chem. Ber.* **1967**, *100*, 228. (e) van Koten, G.; Vrieze, K. *Adv. Organomet. Chem.* **1982**, *21*, 151.

(3) Staal, L. H.; Polm, L. H.; Vrieze, K.; Ploeger, F.; Stam, C. H. *Inorg. Chem.* **1981**, *20*, 3590.

(4) Staal, L. H.; Polm, L. H.; Balk, R. W.; van Koten, G.; Vrieze, K.; Brouwers, A. M. F. *Inorg. Chem.* **1980**, *19*, 3343.

(5) Staal, L. H.; van Koten, G.; Vrieze, K.; van Santen, B.; Stam, C. H. *Inorg. Chem.* **1981**, *20*, 3598.

(6) (a) Keijsper, J.; Polm, L. H.; van Koten, G.; Vrieze, K., to be submitted for publication. (b) When $Ru_3(CO)_{12}$ is reacted with R-DAB (R = *i*-Pr, c-Hx, *i*-Bu, *neo*-Pe, *p*-Tol, di-*i*-Pr-Me) for 0.5 h at 80 °C in toluene or heptane, a blood red solution is obtained. IR spectroscopy indicates the presence of $Ru_3(CO)_{12}$ and $Ru(CO)_3$(R-DAB), which latter species can be isolated and fully characterized for R = di-*i*-Pr-Me only.[3] Upon further reaction the other R derivates react to known $Ru_2(CO)_6$(R-DAB)[4] and succeeding products. Full details will be published soon.

(7) (a) Dyke, A. F.; Knox, S. A. R.; Mead, K. A.; Woodward, P. *J. Chem. Soc., Chem. Commun.* **1981**, 861. (b) Dyke, A. F.; Guerchais, J. E.; Knox, S. A. R.; Roué, J.; Short, R. L.; Taylor, G. E.; Woodward, P. *Ibid.* **1981**, 537. (c) Dyke, A. F.; Knox, S. A. R.; Naish, P. J.; Taylor, G. E. *J. Chem. Soc., Dalton Trans.* **1982**, 1297. (d) Colborn, R. E.; Dyke, A. F.; Knox, S. A. R.; Macpherson, K. M.; Orpen, A. G. *J. Organomet. Chem.* **1982**, *239*, C15.

0020-1669/84/1323-2142$01.50/0

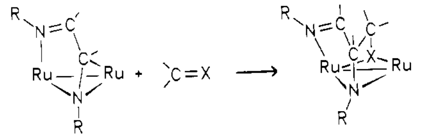

Figure 1. Reaction of 6e-coordinated R-DAB with an unsaturated C=X (X = C,[5] N,[4,6] S[6]) moiety on a diruthenium unit.

it seems much more likely that the reaction sequence is in fact the same for every R and that R determines the thermodynamic and kinetic stability of the intermediates and thus determines the actual products formed. The proposed reaction sequence involves first breakdown of the $Ru_3(CO)_{12}$ cluster to a monomeric species by interaction with R-DAB,[6b] after which a rebuilding, leading to Ru_2–, Ru_3–, or Ru_4–R-DAB complexes, takes place. A crucial intermediate in this process as well as in the reactions of $Ru_2(CO)_6$(R-DAB) with unsaturated molecules (vide supra) is dinuclear $Ru_2(CO)_5$(R-DAB) of which the syntheses, structure, and reactivity are described in this paper.

Experimental Section

Materials and Apparatus. NMR spectra were obtained on a Varian T60 and a Bruker WM 250 spectrometer (^1H) and on a Bruker WP80 apparatus (^{13}C). IR spectra were recorded with a Perkin-Elmer 283 spectrophotometer; mass spectra were obtained with a Varian MAT 771 mass spectrometer applying field desorption technique.[10] Elemental analyses were carried out by the Elemental Analysis Section of the Institute for Applied Chemistry, TNO, Utrecht, The Netherlands. All preparations were carried out under an atmosphere of purified nitrogen, by using carefully dried solvents. Silica gel for column chromatography (60 mesh) was dried and activated before use. R-DAB (R = *i*-Pr, c-Hx, *t*-Bu, *neo*-Pe, *i*-Bu) and Me_3NO have been prepared according to standard procedures.[3,11] $Ru_3(CO)_{12}$ was used as purchased from Strem Chemicals.

Synthesis of $Ru_2(CO)_5$(R-DAB) (2) (R = *i*-Pr, c-Hx). Me_3NO (0.7 mmol) in 0.5 mL of CH_2Cl_2 was added to 0.5 mmol of $Ru_2(CO)_6$(R-DAB) (1) in 30 mL of toluene, prepared in situ.[4] The solution was stirred at room temperature for about 0.5 h. The toluene was evaporated at 60 °C and the residue extracted with 10 mL of diethyl ether. Addition of 15 mL of *n*-pentane and cooling to −70 °C yielded red crystals in about 30% yield. If the complex was used for further reactions, the toluene solution was filtered and used as such. Yield of the complexes in solution was almost quantitative. $Ru_2(CO)_5$(*t*-Bu-DAB) could not be isolated in a similar manner, but after the addition of Me_3NO to a toluene solution of $Ru_2(CO)_6$(*t*-Bu-DAB) its formation could be established with IR and mass spectroscopy (see Table IV).

Alternative Reaction Route. A toluene solution (30 mL) of 0.5 mmol of $Ru_2(CO)_6$(R-DAB) (1) was refluxed for about 6 h until the ν(CO) pattern of $Ru_2(CO)_6$(R-DAB) had disappeared and had been replaced by the characteristic ν(CO) pattern (see Table IV) of the $Ru_2(CO)_5$(R-DAB) (2) products. Work-up procedures were the same as described above.

Synthesis of $Ru_2(CO)_5$(*neo*-Pe-DAB). $Ru_3(CO)_{12}$ (0.33 mmol) and *neo*-Pe-DAB (0.5 mmol) were stirred in 30 mL of toluene or heptane at 60 °C until the solution became intensely red (0.5 h). The solution was refluxed for about 1.5 h and the solvent evaporated. The product was separated by column chromatography. The first green fraction (eluent hexane) contained $Ru_3(CO)_8$(*neo*-Pe-DAB) while the second red/yellow fraction (eluent hexane:ether = 5:1) contained $Ru_2(CO)_5$(*neo*-Pe-DAB). The solvents from the latter fraction were evaporated, and the residue was crystallized from pentane, yielding about 50% of $Ru_2(CO)_5$(*neo*-Pe-DAB). $Ru_2(CO)_5$(*i*-Bu-DAB), which was obtained by refluxing $Ru_3(CO)_{12}$ (0.33 mmol) with *i*-Bu-DAB (0.5 mmol) in 30 mL of toluene, could not be isolated, but its presence in solution was established by IR and mass spectroscopy (see Table IV).

Reactions of $Ru_2(CO)_5$(R-DAB). With CO (R = *i*-Pr, c-Hx, *t*-Bu). CO gas was bubbled through a toluene solution of $Ru_2(CO)_5$(R-DAB) for about 1 min. IR spectroscopy indicated that the ν(CO) pattern of $Ru_2(CO)_5$(R-DAB) (2) was replaced by that of $Ru_2(CO)_6$(R-DAB) (1). The latter species could be isolated in a similar manner as described earlier.[4] Upon reaction of $Ru_2(CO)_5$(R-DAB) (2) (R = *neo*-Pe-, *i*-Bu) with CO, IR spectroscopy indicated that $Ru_2(CO)_6$(R-DAB) (1) was formed though it could not be isolated.

With R-DAB (R = *i*-Pr, c-Hx, *t*-Bu, *neo*-Pe). A toluene solution of $Ru_2(CO)_5$(R-DAB) (2) was stirred with a slight excess of R-DAB at 100 °C until the ν(CO) pattern of $Ru_2(CO)_5$(R-DAB) was replaced (30 min) by that of $Ru_2(CO)_5$(R-IAE)[4] (3) (R = *i*-Pr, c-Hx, *t*-Bu). Similar reaction of $Ru_2(CO)_5$(*neo*-Pe-DAB) with *neo*-Pe-DAB yielded the earlier inaccessible $Ru_2(CO)_4$(*neo*-Pe-DAB)$_2$ (3′). The workup procedures and yields for all species were the same as described in the literature[4] for analogous compounds, and the products were identified by IR, ^1H NMR, and mass spectroscopy.

By Thermal Decomposition (R = *i*-Pr, c-Hx, *neo*-Pe). A heptane or octane solution of $Ru_2(CO)_5$(R-DAB) (2) was refluxed for about 8 h. After cooling, $Ru_4(CO)_8$(R-DAB)$_2$ (4) precipitated and could be isolated as described earlier.[4] Yields were almost quantitative (>80%), including the case of R = *neo*-Pe.

With $Fe_2(CO)_9$ (R = *i*-Pr, c-Hx, *t*-Bu). A freshly prepared toluene solution of $Ru_2(CO)_5$(R-DAB) (2) was stirred with 1 equiv of $Fe_2(CO)_9$ for about 0.5 h at 50 °C. The residue obtained by evaporation of both toluene and formed $Fe(CO)_5$ was purified by column chromatography using hexane as eluent. Crystallization for R = *i*-Pr from pentane yielded 60% (based on *i*-Pr-DAB) of red crystals, which were identified as $FeRu(CO)_6$(*i*-Pr-DAB) (5) by analysis and IR, mass, and NMR spectroscopy (see Tables IV and V). No other Ru–carbonyl product was observed. $FeRu(CO)_6$(R-DAB) (R = c-Hx, *t*-Bu) could not be isolated, but its formation was established in solution by IR and mass spectroscopy.

With $Ru_3(CO)_{12}$ (R = *neo*-Pe). A toluene solution of 0.5 mmol of $Ru_2(CO)_5$(*neo*-Pe-DAB) was refluxed for about 2 h with 0.25 mmol of $Ru_3(CO)_{12}$ until the color of the solution had changed to green and the ν(CO) pattern of $Ru_2(CO)_5$(*neo*-Pe-DAB) (2) had disappeared. The reaction mixture was purified by column chromatography, using hexane–diethyl ether (5:1) as eluent. Crystallization at −20 °C from pentane yielded green crystals in about 70% yield, which were identified as $Ru_3(CO)_8$(*neo*-Pe-DAB) (6) by analysis and IR, mass, and ^1H NMR spectroscopy (see Tables IV and V). $Ru_3(CO)_8$(*i*-Bu-DAB) could not be obtained in a similar manner because of the inaccessibility of $Ru_2(CO)_5$(*i*-Bu-DAB) but could be isolated by refluxing $Ru_3(CO)_{12}$ (0.33 mmol) for 3 h with 0.33 mmol of *i*-Bu-DAB. The workup procedure was the same as that described for $Ru_3(CO)_8$(*neo*-Pe-DAB) (30% yield).

Crystal Structure Determination of $Ru_2(CO)_5$(*i*-Pr-DAB), (1,4-Diisopropyl-1,4-diaza-1,3-butadiene)pentacarbonyldiruthenium, $C_{13}H_{16}N_2O_5Ru_2$. Crystals of the title compound were orthorhombic, space group $P2_12_12_1$. The unit cell had the dimensions a = 12.775 (2) Å, b = 13.518 (3) Å, c = 9.636 (10) Å, Z = 4, V = 1664.1 Å^3, and d_{calcd} = 1.93 g·cm^{-3}. The crystal was sealed in a capillary under nitrogen, and a total of 1503 independent reflections with $\theta < 65°$ were measured on a Nonus CAD 4 diffractometer using graphite-monochromated Cu Kα radiation (μ = 152.9 cm^{-1}). Of these reflections, 23 were below the $2.5\sigma(I)$ level and were treated as unobserved. No absorption correction was applied. The Ru positions were derived from an E^2 Patterson synthesis. A subsequent F_o synthesis revealed the remaining non-hydrogen atoms. Refinement proceeded by means of anisotropic block-diagonal least-squares calculations. The final R value was 0.045 (R_w = 0.064). A weighting scheme $w = 1/(2.1 + F_o + 0.023F_o^2)$ was employed, and the anomalous scattering of Ru was taken into account.[12a] In the final ΔF synthesis effects around Ru due to absorption were of the order of 1 e/Å^3. Refinement of the inverted structure led to R = 0.053, so the structure as given represents the correct configuration. The computer programs used for plotting[12b]

---

(8) Staal, L. H.; van Koten, G.; Vrieze, K. *J. Organomet. Chem.* **1981**, *206*, 99.

(9) Gast, C. H.; Kraak, J. C.; Staal, L. H.; Vrieze, K. *J. Organomet. Chem.* **1981**, *208*, 225.

(10) Staal, L. H.; van Koten, G.; Fokkens, R. H.; Nibbering, N. M. M. *Inorg. Chim. Acta* **1981**, *50*, 205 and references therein.

(11) (a) tom Dieck, H.; Renk, I. W. *Chem. Ber.* **1971**, *104*, 92. (b) Lecher, H. Z.; Hardy, W. B. *J. Am. Chem. Soc.* **1948**, *70*, 3789.

(12) (a) "International Tables for X-ray Crystallography"; Kynoch Press: Birmingham, England, 1964; Vol. III. (b) Motherwell, S.; Clegg, B. "PLUTO, Program for Plotting Molecular and Crystal Structures"; University of Cambridge: England, 1978. (c) Colton, R.; McCormick, M. J. *Coord. Chem. Rev.* **1980**, *31*, 1.

Table I. Final Atomic Coordinates (Esd) of $Ru_2(CO)_5$(*i*-Pr-DAB)

	x	*y*	*z*
Ru(1)	0.41651 (6)	0.47604 (6)	0.67260 (8)
Ru(2)	0.59204 (5)	0.37932 (5)	0.76381 (9)
O(1)	0.2696 (8)	0.6206 (8)	0.8130 (11)
O(2)	0.3833 (9)	0.5959 (8)	0.4129 (11)
O(3)	0.6092 (8)	0.5997 (7)	0.7658 (13)
O(4)	0.7034 (8)	0.3798 (11)	1.0384 (9)
O(5)	0.8122 (8)	0.3712 (9)	0.6498 (11)
N(1)	0.4356 (7)	0.3558 (7)	0.8358 (9)
N(2)	0.5033 (7)	0.3470 (7)	0.5804 (9)
C(1)	0.3262 (9)	0.5645 (9)	0.7638 (14)
C(2)	0.3955 (10)	0.5515 (9)	0.5132 (13)
C(3)	0.5659 (9)	0.5270 (9)	0.7462 (13)
C(4)	0.6613 (9)	0.3807 (10)	0.9328 (14)
C(5)	0.7261 (10)	0.3764 (10)	0.6889 (12)
C(6)	0.3614 (8)	0.3224 (8)	0.7355 (13)
C(7)	0.3970 (9)	0.3176 (7)	0.5992 (13)
C(8)	0.3942 (9)	0.3619 (9)	0.9784 (12)
C(9)	0.4302 (11)	0.4562 (11)	1.0539 (13)
C(10)	0.4194 (14)	0.2695 (12)	1.0601 (15)
C(11)	0.5357 (9)	0.3419 (9)	0.4341 (12)
C(12)	0.5777 (14)	0.2398 (13)	0.4034 (15)
C(13)	0.6171 (11)	0.4218 (11)	0.3986 (14)

Table II. Bond Lengths (Esd) (Å) of $Ru_2(CO)_5$(*i*-Pr-DAB)

	Around Ru		
Ru(1)-Ru(2)	2.741 (1)	Ru(1)-C(7)	2.27 (1)
Ru(1)-N(1)	2.27 (1)	Ru(2)-N(1)	2.14 (1)
Ru(1)-N(2)	2.25 (1)	Ru(2)-N(2)	2.14 (1)
Ru(1)-C(1)	1.88 (1)	Ru(2)-C(3)	2.03 (1)
Ru(1)-C(2)	1.86 (1)	Ru(2)-C(4)	1.85 (1)
Ru(1)-C(3)	2.15 (1)	Ru(2)-C(5)	1.86 (1)
Ru(1)-C(6)	2.28 (1)		
	Within the Ligand		
N(1)-C(6)	1.43 (1)	C(8)-C(9)	1.54 (2)
N(1)-C(8)	1.47 (1)	C(8)-C(10)	1.51 (2)
N(2)-C(7)	1.43 (1)	C(11)-C(12)	1.51 (2)
N(2)-C(11)	1.47 (1)	C(11)-C(13)	1.54 (2)
C(6)-C(7)	1.39 (2)		
	Within the Carbonyls		
C(1)-O(1)	1.15 (2)	C(4)-O(4)	1.15 (2)
C(2)-O(2)	1.15 (2)	C(5)-O(5)	1.16 (2)
C(3)-O(3)	1.14 (1)		

Table III. Selected Bond Angles (Esd) (deg) within $Ru_2(CO)_5$(*i*-Pr-DAB)

	Metal Carbonyl		
Ru(2)-Ru(1)-C(3)	47.2 (4)	Ru(2)-C(3)-O(3)	138.7 (10)
Ru(1)-Ru(2)-C(3)	50.9 (3)	Ru(1)-C(3)-Ru(2)	81.9 (4)
Ru(1)-C(3)-O(3)	139.4 (10)	Ru-C-O(terminal)	177 (1) (mean)[a]
	Metal Ligand		
N(1)-Ru(1)-N(2)	70.5 (3)	Ru(1)-N(2)-Ru(2)	77.1 (3)
N(1)-Ru(2)-N(2)	75.1 (3)	C(6)-Ru(1)-C(7)	35.7 (4)
Ru(1)-N(1)-Ru(2)	76.7 (3)		
	Ligand		
N(1)-C(6)-C(7)	115.9 (9)	C(6)-N(1)-C(8)	114.2 (9)
C(6)-C(7)-N(2)	114.7 (10)	C(7)-N(2)-C(11)	112.1 (9)

[a] The esd of the mean value has been calculated by $(\Sigma_i(x_i - \bar{x})^2/N)^{1/2}$

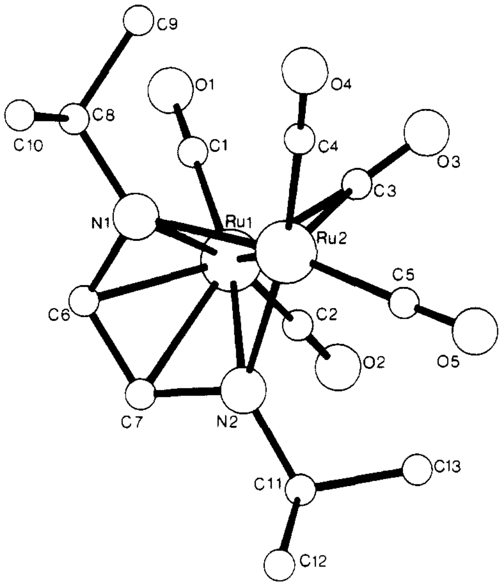

Figure 2. Molecular geometry of and atomic numbering in $Ru_2(CO)_5$(*i*-Pr-DAB).

Table IV. IR and FD Mass Spectral Data

compd	m_{obsd} (m_{calcd})[a]	ν(CO), cm^{-1}
$Ru_2(CO)_5$(R-DAB) (2)		
R = *i*-Pr	483 (482.42)	2030, 1998, 1960, 1943, 1842[b]
c-Hx	563 (562.55)	2030, 1997, 1957, 1941, 1841[b]
t-Bu	510 (510.47)	2021, 1990, 1947, 1931, 1832[c]
neo-Pe	539 (538.52)	2034, 2002, 1964, 1950, 1838[b]
i-Bu	510 (510.47)	2033, 2000, 1965, 1949, 1841[b]
$Ru_2(CO)_4(R\text{-}DAB)_2$ (3′)		
R = *neo*-Pe	707 (706.84)	1971, 1904[d]
$FeRu(CO)_6$(R-DAB) (5)		
R = *i*-Pr	466 (465.21)	2070, 2008, 1999, 1986, 1939[b]
c-Hx	545 (545.34)	2067, 2005, 1998, 1985, 1937[b]
t-Bu	494 (493.26)	2064, 2004, 1995, 1983, 1939[b]
$Ru_3(CO)_8$(R-DAB) (6)		
R = *neo*-Pe	725 (723.62)	2082, 2023, 2005, 1998 (sh), 1975, 1947, 1923[b]
i-Bu	*e* (695.57)	2083, 2024, 2007, 1996 (sh), 1975, 1947, 1923[b]
$Ru_2(CO)_5$(R-IAE) (3)	*f*	*f*
$Ru_4(CO)_8(R\text{-}DAB)_2$ (4)	*f*	*f*

[a] The calculated *m* values are based upon ^{101}Ru; the observed *m* values account for the highest peak of the isotope pattern. [b] In hexane. [c] In toluene. [d] In dichloromethane. [e] Not measured. [f] Identical with reported literature values.[3,4]

the scattering factors and dispersion corrections[12a] were taken from the literature. The molecular geometry of $Ru_2(CO)_5$(*i*-Pr-DAB) with the numbering of the atoms is shown in Figure 2, which shows a PLUTO drawing[12b] of the molecule. Atomic parameters, bond lengths, and selected bond angles are given in Tables I–III, respectively. All bond angles, anisotropic thermal parameters, and a list of the observed and calculated structure factors are included with the supplementary material.

Analytical Data. All complexes gave satisfactory results (supplementary material). The complexes showed characteristic ν(C═O) IR absorptions, which are listed in Table IV. Mass spectra have been recorded by using the field desorption (FD) technique. Observed and calculated *m*/*z* values are also listed in Table IV.

Results

Molecular Structure. The molecular geometry of $Ru_2(CO)_5$(*i*-Pr-DAB) is shown in Figure 2. There is an almost perfect mirror plane in the molecule through Ru(1)C(3)Ru(2) (Figure 3). The Ru(1)–Ru(2) distance of 2.741 (1) Å is normal for CO-bridged dimeric Ru compounds.[6,7] In these complexes, Ru–Ru distances were found between 2.70 and 2.75 Å.

The metal carbonyl unit consists of four terminal and one bridging CO groups. The four terminal carbonyls are located

Table V. ^1H NMR Data[a]

compd	R group[b]	imine H
$Ru_2(CO)_5$(R-DAB) (2)		
R = *i*-Pr	2.13 (sept,[c] 2 H), 1.01 (d,[c] 6 H)/0.92 (d,[c] 6 H)	6.00 (s, 2 H)
c-Hx	2.11 (br m, 2 H), 2–1 (br 20 H)	6.06 (s, 2 H)
neo-Pe	2.77 (d,[e] 2 H)/2.25 (d,[e] 2 H), 0.96 (s, 18 H)	6.03 (s, 2 H)
$Ru_2(CO)_4(R\text{-DAB})_2$[d] (3′)		
R = *neo*-Pe	3.45 (d,[e] 1 H)/3.36 (d,[e] 1 H), 1.09 (s, 2 H), 3.08 (d,[f] 1 H)/2.33 (d,[f] 1 H), 0.97 (s, 9 H)	8.14 (d,[g] 1 H), 5.03 (d,[g] 1 H)
$Ru_4(CO)_8(R\text{-DAB})_2$[d] (4)		
R = *neo*-Pe	2.66 (d,[e] 2 H)/2.32 (d,[e] 2 H), 1.08 (s, 18 H)	6.43 (s, 2 H)
$FeRu(CO)_6$(R-DAB)[h] (5)		
R = *i*-Pr	3.11 (sept,[c] 1 H), 2.88 (sept,[c] 1 H), 1.50 (d,[c] 3 H)/1.39 (d,[c] 3 H), 0.95 (d,[c] 6 H)	7.00 (d,[g] 1 H), 2.93 (d,[g] 1 H)
$Ru_3(CO)_8$(R-DAB) (6)		
R = *neo*-Pe	3.85 (d,[e] 2 H)/2.67 (d,[e] 2 H), 1.05 (s, 18 H)	5.64 (s, 2 H)
i-Bu	3.77 (d[c] of d,[e] 2 H)/2.58 (d[c] of d,[e] 2 H), 1.88 (m, 2 H), 1.09 (d,[c] 6 H)/0.86 (d,[c] 6 H)	5.51 (s, 2 H)

[a] The values (ppm relative to Me_4Si) have been obtained in toluene-d_8 solutions. [b] Vertical bars separate diastereotopic pairs; s = singlet, d = doublet, br = broad, sept = septet. [c] $J = 6$ Hz. [d] In $CDCl_3$. [e] $J = 12$ Hz. [f] $J = 14$ Hz. [g] $J = 2$ Hz. [h] ^{13}C NMR (in toluene-d_8, referenced to Me_4Si): 216.7, 205.3, 198.3, 188.3 (CO); 67.4, 65.4 (N–C(*i*-Pr)); 28.0/27.6, 23.5 (CH_3(*i*-Pr)); 175.8 (imine C); 61.4 (amine C).

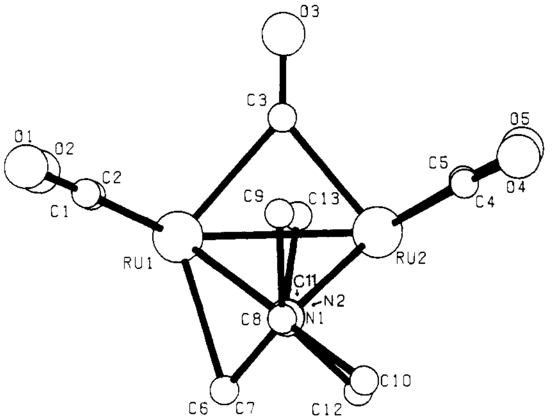

Figure 3. Molecular structure of $Ru_2(CO)_5$(*i*-Pr-DAB) projected on Ru(1)C(3)Ru(2), which shows the symmetry in the molecule.

symmetrically on the two Ru atoms (see Figure 3) with equal bond lengths: Ru–C(terminal) = 1.86 (1) Å (mean); C–O-(terminal) = 1.15 (2) Å (mean). The bridging carbonyl is bonded via C(3) to Ru(1) and Ru(2) with bond lengths of 2.15 (1) and 2.03 (1) Å, respectively, while the C(3)–O(3) vector is almost perpendicular to the Ru(1)–Ru(2) vector (87°), indicating that this carbonyl is asymmetrically bridging the Ru–Ru bond.[12c]

The N(1)C(6)C(7)N(2) part of the ligand is flat with N(1)–C(8) and N(2)–C(11) only slightly bent out of the plane (<1.5°). Ru(2) deviates a little from the plane with a dihedral angle between N(1)Ru(2)N(2) and the N(1)C(6)C(7)N(2) plane of 6.5°. Values of 14[13] and 10.0°[14] have been reported for other dinuclear species containing 8e-bonded R-DAB.

The four central DAB atoms, N(1), C(6), C(7), and N(2), are located an equal distance from Ru(1) of 2.27 (1) Å (mean). This is significantly longer than the distance between the N atoms and Ru(2) of 2.14 (1) Å. This orientation of the R-DAB ligand was observed earlier in $Ru_4(CO)_8(i\text{-Pr-DAB})_2$[3] and $Ru_2(CO)_4(i\text{-Pr-DAB})(\mu\text{-}C_2H_2)$[13] in which the *i*-Pr-DAB ligand is in the 8e-coordination mode, and it indicates that in the present compound N(1) and N(2) are chelate bonded to Ru(2) and that N(1)═C(6) and N(2)═C(7) are η^2-bonded to Ru(1).

Accordingly, the bond lengths in the DAB part of the *i*-Pr-DAB-ligand are N═C = 1.43 (1) Å (mean) and central C(6)–C(7) = 1.39 (2) Å. In free c-Hx-DAB these distances are 1.258 (3) and 1.457 (3) Å, respectively.[15] Comparison of these bond lengths indicates that in $Ru_2(CO)_5$(*i*-Pr-DAB) the LUMO of the R-DAB ligand, which has bonding character between the two central C atoms and is antibonding between the C and N atoms,[2d,15] is extensively occupied. This results in the long C═N and the short C–C distances observed. The type of bonding and the distances within the ligand are very similar to those of isoelectronic 1,3-butadiene in $M_2(CO)_6$(1,3-butadiene) (M = Fe, Ru), in which the outer C atoms are σ bonded to M(2), while the C^α═C^β double bonds are both η^2 coordinated to M(1).[16]

IR: ν(CO) Region. All $Ru_2(CO)_5$(R-DAB) complexes show characteristic absorption patterns in the ν(CO) region (see Table IV). They have four strong bands between 2040and 1930 cm^{-1} due to the terminal CO groups and one medium band around 1840 cm^{-1}, which can be assigned to the bridging carbonyl. The complexes (R = *i*-Pr, c-Hx, *t*-Bu, *neo*-Pe, *i*-Bu) give comparable spectra, indicating similar metal carbonyl parts. The spectra also closely resemble those of $Ru_2(CO)_5$(R-DAB-L), in which L is a ligand linked to R-DAB via a C–C bond[5,6a] (see Introduction). These species all contain the same $(\mu\text{-CO})[(CO)_2Ru]_2$ fragment.

FD Mass Spectrometry. Field desorption mass spectrometry has proved itself to be a valuable method for the characterization of organometallic species with low stability and/or low volatility. The molecular ion is nearly always generated exclusively, i.e. no further fragmentation occurs.[10] Also in this study FD mass spectrometry appeared to be an excellent method for the identification of the new products. The results are summarized in Table IV and are in agreement with the calculated molecular weights.

^{1}H NMR Spectroscopy. The ^1H NMR data are listed in Table V. In free R-DAB the imine protons absorb between 7 and 9 ppm, while this resonance position is hardly affected if only σ-N coordination is present.[17,2e] If, on the other hand, R-DAB also uses its π electrons for coordination, then the imine protons are shifted drastically upfield. Thus, in 6e(σ-N, σ-N′, η^2-C═N′ or σ-N, μ^2-N′, η^2-C═N′)-coordinated R-DAB complexes, the imine protons are no longer equivalent and an AX pattern is observed.[3,4,18] The imine proton of the σ-N-

---

(13) Staal, L. H.; van Koten, G.; Vrieze, K.; Ploeger, F.; Stam, C. H. *Inorg. Chem.* **1981**, *20*, 1830.

(14) Adams, R. D. *J. Am. Chem. Soc.* **1980**, *102*, 7476.

(15) Keijsper, J.; van der Poel, H.; Polm, L. H.; van Koten, G.; Vrieze, K.; Seignette, P. F. A. B.; Varenhorst, R.; Stam, C. H. *Polyhedron*, in press.

(16) (a) Astier, A.; Daran, J. C.; Jeannin, Y.; Rigault, C. *J. Organomet. Chem.* **1983**, *241*, 53 and references therein. (b) Cotton, F. A. *Prog. Inorg. Chem.* **1976**, *21*, 1.

(17) tom Dieck, H.; Renk, I. W.; Franz, K. D. *J. Organomet. Chem.* **1975**, *94*, 417.

coordinated C=N part still absorbs at about 8 ppm, but the proton of the η^2-C=N-coordinated half appears at about 4 ppm, with J_{AX} = 2 Hz. In 8e(σ-N, σ-N′, η^2-C=N, η^2-C′=N′)-coordinated R-DAB compounds, both imine protons are again equivalent and give one singlet at about 6 ppm.[3,13] In $Ru_2(CO)_5$(R-DAB) complexes the observation of one singlet at 6.0 ppm for both the imine protons and the one pattern for the two R groups proves that the halves of the R-DAB ligand are equivalent and that the 8e-bonding mode, as found in the solid state, is retained in solution.

Reactions of $Ru_2(CO)_5$(R-DAB) (See Also Figure 5). With CO (R = *i*-Pr, c-Hx, *t*-Bu, *neo*-Pe, *i*-Bu). $Ru_2(CO)_5$(R-DAB) (**2**) reacts with CO according to eq 1.

$$\mathrm{Ru_2(CO)_5(R\text{-}DAB) + CO \rightarrow \underset{\mathbf{1}}{Ru_2(CO)_6(R\text{-}DAB)}} \quad (1)$$

With R-DAB (R = *i*-Pr, c-Hx, *t*-Bu, *neo*-Pe). $Ru_2(CO)_5$(R-DAB) reacts with R-DAB according to eq 2. For R = *neo*-Pe, only $Ru_2(CO)_4$(*neo*-Pe-DAB)$_2$ could be obtained in a similar manner as described earlier for comparable compounds with other R groups. Their IR, mass, and ^{1}H NMR spectral data are comparable with those of other $Ru_2(CO)_4$(R-DAB)$_2$ products and are included in Tables IV and V.

$$\mathrm{Ru_2(CO)_5(R\text{-}DAB) + R\text{-}DAB \rightarrow \underset{\mathbf{3}}{Ru_2(CO)_5(R\text{-}IAE)} \xrightarrow[-CO]{\Delta T = 120\ ^\circ C} \underset{\mathbf{3'}}{Ru_2(CO)_4(R\text{-}DAB)_2}} \quad (2)^4$$

By Thermal Decomposition (R = *i*-Pr, c-Hx, *neo*-Pe). When heated in octane, $Ru_2(CO)_5$(R-DAB) (**2**) reacts to give $Ru_4(CO)_8$(R-DAB)$_2$ (**4**) according to eq 3. 250-MHz ^{1}H NMR data indicate that also for R = *neo*-Pe the butterfly-like molecule $Ru_4(CO)_8$(R-DAB)$_2$ is in the fast exchange as a result of the "flying" motion of the Ru_4 skeleton.[3]

$$\mathrm{2Ru_2(CO)_5(R\text{-}DAB) \rightarrow Ru_4(CO)_8(R\text{-}DAB)_2 + 2CO} \quad (3)$$

With $Fe_2(CO)_9$ (R = *i*-Pr, c-Hx, *t*-Bu). $Ru_2(CO)_5$(R-DAB) reacts with $Fe_2(CO)_9$ according to eq 4. The relative intensities of the ν(CO) peaks of $FeRu(CO)_6$(R-DAB) (R = *i*-Pr, c-Hx, *t*-Bu) are the same as those of $M_2(CO)_6$(R-DAB) (M = Fe, Ru),[2a,4] but the peak positions have changed markedly. ^{1}H NMR spectroscopy (Table V) revealed an AX pattern for the imine protons and an inequivalence of the *i*-Pr groups in $FeRu(CO)_6$(*i*-Pr-DAB). This is in line with a 6e-(σ-N, μ^2-N′, η^2-C=N′) coordination mode, with the DAB ligand bridging the two metals, just as in homodinuclear $M_2(CO)_6$(R-DAB) (M = Fe, Ru).[2a,4] Included in Table V are the ^{13}C NMR absorptions for $FeRu(CO)_6$(*i*-Pr-DAB). The different chemical shifts for both the imine carbons and the *i*-Pr groups agree well with the proposed coordination mode.[19] In Figure 4, the low-field part of the spectrum is given.

$$\mathrm{Ru_2(CO)_5(R\text{-}DAB) + Fe_2(CO)_9 \rightarrow \underset{\mathbf{5}}{FeRu(CO)_6(R\text{-}DAB)} + Fe(CO)_5 + decomposition\ products} \quad (4)$$

The three sharp singlets at 205.3, 198.3, and 188.2 ppm correspond to a rigid $Ru(CO)_3$ unit. The singlet at 216.7 ppm is assigned to the three rapidly scrambling CO groups on the Fe atom.[12,19] It was observed that this signal broadened at −60 °C (intermediate exchange), but the slow-exchange limit could not be reached.

From these spectroscopic measurements on $FeRu(CO)_6$(R-DAB) it is impossible to conclude toward which metal atom R-DAB is η^2-C=N coordinated, though we believe (see Discussion) that it is σ-N coordinated to Ru and η^2-C=N coordinated to Fe (M = Ru, M′ = Fe in Figure 5).

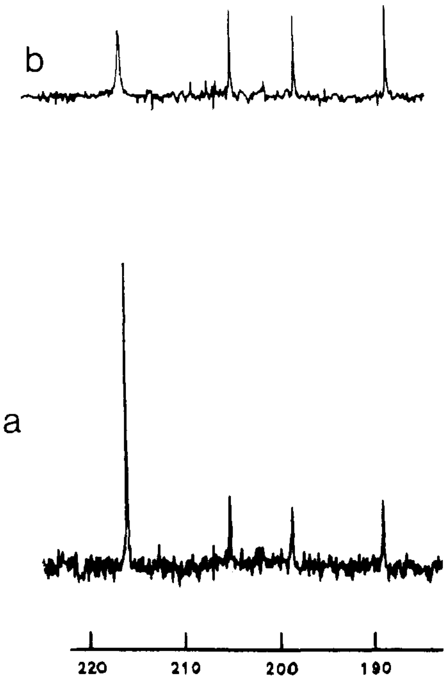

Figure 4. CO part of the ^{13}C NMR spectrum of $FeRu(CO)_6$(*i*-Pr-DAB): (a) *T* = 40 °C, fast exchange on Fe; (b) *T* = −60 °C, intermediate exchange on Fe.

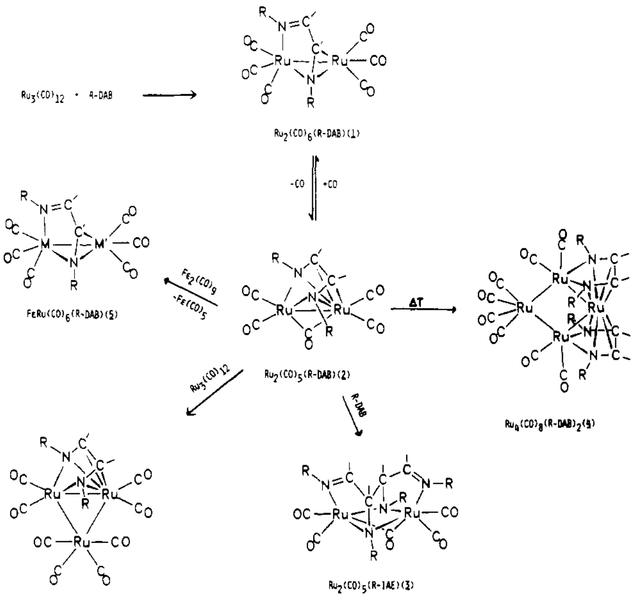

Figure 5. Formation and reactivity of $Ru_2(CO)_5$(R-DAB). In compound **5**, $FeRu(CO)_6$(R-DAB), M probably is Ru and M′ is Fe (see text).

With $Ru_3(CO)_{12}$ (R = *neo*-Pe, *i*-Bu). $Ru_2(CO)_5$(R-DAB) (isolated for R = *neo*-Pe, observed in solution for R = *i*-Bu) reacts with $Ru_3(CO)_{12}$ according to eq 5.

$$\mathrm{Ru_2(CO)_5(R\text{-}DAB) + Ru_3(CO)_{12} \rightarrow \underset{\mathbf{6}}{Ru_3(CO)_8(R\text{-}DAB)} + decomposition\ products} \quad (5)$$

---

(18) Staal, L. H.; Keijsper, J.; van Koten, G.; Vrieze, K.; Cras, J. A.; Bosman, W. P. *Inorg. Chem.* **1981**, *20*, 555.

(19) Staal, L. H.; Keijsper, J.; Polm, L. H.; Vrieze, K. *J. Organomet. Chem.* **1981**, *204*, 101 and references cited therein.

IR spectroscopy on the green trinuclear product in the ν(CO) region only shows strong and very strong absorptions between 2090 and 1920 cm^{-1}, indicating that all the carbonyls are terminal (see Table IV). The ^1H NMR results for $Ru_3(CO)_8$(R-DAB) (**6**) (see Table V) reveal that in these compounds R-DAB is coordinated in a 8e(σ-N, σ-N′, η^2-C=N, η^2-C′=N′) bonding mode. The most probable structure, which is in agreement with the symmetry of the molecule, as evidenced by ^1H NMR, is shown in Figure 5. This molecule can be interpreted as being derived from the starting compound $Ru_2(CO)_5$(R-DAB) by substituting the bridging carbonyl for the likewise 2e-donating $Ru(CO)_4$ unit.

Discussion

Reaction Sequence. With $Ru_2(CO)_5$(R-DAB) (**2**) we have isolated a crucial intermediate in the Ru–carbonyl–R-DAB reaction sequence,[6b] and this isolation makes it possible to synthesize species, which were earlier inaccessible (e.g., $Ru_2(CO)_4$(*neo*-Pe-DAB$)_2$[4]) or accessible only in a very low yield (e.g., $Ru_4(CO)_8$(*neo*-Pe-DAB$)_2$[3]). Earlier tentative suggestions[3,8,9] about the Ru–carbonyl–R-DAB reaction sequence implied a gradual breakdown of the $Ru_3(CO)_{12}$ cluster, which would stop, depending on R, when the most stable complex was found. (See Introduction.) This could be either a trinuclear, dinuclear, or mononuclear species. We now have firm evidence, however, that for all R groups the reaction sequence is the same: a complete breakdown of the Ru_3 cluster to a monomeric Ru–carbonyl–R-DAB species appears to be the first detectable step,[6b] which is most probably preceded by coordination of R-DAB to the Ru_3 cluster. This step, however, cannot be observed. The formation of the monomeric Ru species is followed by the formation of $Ru_2(CO)_6$(R-DAB) (**1**) and subsequently $Ru_2(CO)_5$(R-DAB) (**2**). That $Ru_2(CO)_5$(R-DAB) is the key intermediate is indeed supported by its reactivity pattern. It reacts to either trinuclear $Ru_3(CO)_8$(R-DAB) (**6**) (for R = *neo*-Pe, *i*-Bu), if excess $Ru_3(CO)_{12}$ is present,[20a] or to dinuclear $Ru_2(CO)_5$(R-IAE) (**3**) (for R = *i*-Pr, c-Hx, *t*-Bu, *neo*-Pe) and subsequently[4] $Ru_2(CO)_4$(R-DAB$)_2$ (**3′**), if excess R-DAB is present.

Furthermore, when CO is present it gives rise to the formation of dinuclear $Ru_2(CO)_6$(R-DAB) (**1**) (for R = *i*-Pr, c-Hx, *t*-Bu, *neo*-Pe, *i*-Bu) or tetranuclear $Ru_4(CO)_8$(R-DAB$)_2$ (**4**) (for R = *i*-Pr, c-Hx, *neo*-Pe) when it is heated in octane. The formation and reactivity of $Ru_2(CO)_5$(R-DAB) is illustrated in Figure 5.

Complex Formation. $Ru_2(CO)_5$(R-DAB) is formed out of $Ru_2(CO)_6$(R-DAB) by dissociation of a CO group, which is achieved by heating or by reaction with Me_3NO. $Ru_2(CO)_5$(R-DAB) is stable in toluene but decomposes quickly in chlorinated solvents. IR spectra suggest that also for R = *i*-Bu and *neo*-Pe $Ru_2(CO)_5$(R-DAB) is formed subsequent to $Ru_2(CO)_6$(R-DAB). During the reaction the R-DAB ligand changes its coordination mode from the 6e(σ-N, μ^2-N′, η^2-C=N′) to the 8e(σ-N, σ-N′, η^2-C=N, η^2-C′=N′) one, so that the EAN rule is obeyed in both the starting and the reaction product. The flexibility of the R-DAB ligand in accommodating its coordination made to the number of carbonyls present was also observed in the reaction of $CoMn(CO)_7$(R-DAB) to $CoMn(CO)_6$(R-DAB), in which reaction the coordination mode changed from the 4e to the 6e one.[18]

Reactivity. The reactions of $Ru_2(CO)_5$(R-DAB) with CO, R-DAB, and $Fe_2(CO)_9$ as well as the thermal decomposition reaction all have in common that during the reaction at least one η^2-C=N to Ru(1) bond must have been broken (see Figure 5).

A possible mechanism is an interaction between the new incoming moiety and the $Ru_2(CO)_5$(R-DAB) molecule, which forces one η^2-C=N unit to dissociate from Ru(1) while at the same time the new moiety coordinates to Ru(1) and an intramolecular rearrangement yields the final product. Another, maybe more likely, possibility is the existence in solution of an equilibrium between the 8e(σ-N, σ-N′, η^2-C=N, η_2-C′=N′) and an unsaturated 6e(σ-N, σ-N′, η^2-C′=N′) bonded R-DAB species. When the R-DAB ligand is in the 6e coordination mode, a 2e-donor ligand may add in a fast step to Ru(1) after which an intramolecular rearrangement yields the final product. Thus, according to this mechanism, in the rapid reaction of $Ru_2(CO)_5$(R-DAB) (**2**) with CO, yielding the parent carbonyl $Ru_2(CO)_6$(R-DAB) (**1**), one η^2-C=N unit would dissociate from Ru(1) and CO would add to Ru(1). An intramolecular rearrangement then changes the coordination mode of R-DAB from 6e(σ-N, σ-N′, η^2-C=N′) to 6e(σ-N, μ^2-N′, η^2-C=N′) while the bridging carbonyl becomes terminal on Ru(2). The crystal structure of $CoMn(CO)_6$(*t*-Bu-DAB),[18] with its semibridging CO group and its DAB ligand, coordinated between the two extreme 6e modes, provides a view for this last rearrangement process.

In the reaction of $Ru_2(CO)_5$(R-DAB) (**2**) with R-DAB, yielding $Ru_2(CO)_5$(R-IAE) (**3**) and consequently[4] $Ru_2(CO)_4$(R-DAB$)_2$ (**3′**), dissociation of one η^2-C=N unit is probably followed by coordination of one N atom of the incoming R-DAB ligand to Ru(1). This ligand is then within close distance of the originally, now 6e, coordinated R-DAB, and the C–C coupling can occur after which a subsequent rearrangement reaction yields the final product. (See Figure 5.)

Two Ru–η^2-C=N bonds must have been broken in the thermal decomposition reaction with concomitant loss of CO, yielding $Ru_4(CO)_8$(R-DAB$)_2$ (**4**) quantitatively. The precise mechanism, however, remains unclear. The product can be envisaged as a dimerization product of two $Ru_2(CO)_4$(R-DAB) fragments.[20b]

In the reaction of $Ru_2(CO)_5$(R-DAB) with the metal carbonyls $Fe_2(CO)_9$ and $Ru_3(CO)_{12}$, the first step after the dissociation of the η^2-C=N unit is very likely to be an addition of a $M(CO)_4$ unit to Ru(1). The resulting $Ru_2M(CO)_9$(R-DAB) reacts to $Ru_3(CO)_8$(R-DAB)[21] (M = Ru) or $FeRu(CO)_6$(R-DAB) (**5**). The isolation of $Ru_3(CO)_9$(R-DAB) and crystal structure for R = c-Hx provide a firm basis for this thesis.[6]

From spectroscopic measurements it is impossible to conclude to which atom R-DAB is η^2-C=N coordinated in $FeRu(CO)_6$(R-DAB). We anticipate, however, that because of the relative ease of η^2-C=N dissociation and the mild reaction conditions employed, R-DAB is η^2-C=N coordinated to Fe; i.e., M′ = Fe and M = Ru in Figure 5.

Further reactions of $Ru_2(CO)_5$(R-DAB) with metal carbonyls and unsaturated molecules such as acetylenes, allenes, and olefins, are currently being investigated.

Conclusions

It has been shown that $Ru_2(CO)_5$(R-DAB) is a very reactive species and a key intermediate in the Ru–carbonyl–R-DAB reaction sequence. It can react with CO, R-DAB, and $Ru_3(CO)_{12}$, yielding an addition product [$Ru_2(CO)_6$(R-DAB) (**1**)],

---

(20) (a) We have IR evidence that also in the reaction of $Ru_2(CO)_5$(R-DAB) (R = *i*-Pr, c-Hx) with $Ru_3(CO)_{12}$ $Ru_3(CO)_8$(R-DAB) is formed, but these species could not be isolated. (b) A reviewer suggested that $Ru_4(CO)_8$(R-DAB$)_2$ might be formed through addition of a mononuclear unit to $Ru_3(CO)_8$(R-DAB) because this process would require less rearrangement than the dimerization process. However, for R = *neo*-Pe, isolated $Ru_3(CO)_8$(R-DAB) does not react with $Ru_3(CO)_{12}$ to yield $Ru_4(CO)_8$(R-DAB$)_2$. Therefore, a dimerization reaction seems to us more probable than the addition reaction suggested.

(21) $Ru_3(CO)_8$(R-DAB), which is the counterpart of $Ru_2(CO)_5$(R-DAB) through replacement of a bridging carbonyl with the likewise 2e-donating bridging $Ru(CO)_4$ unit, also shows an exciting chemistry in reactions with CO, CH_2N_2, acetylenes, and other small molecules, on which we will report soon.

a product in which two R-DAB's are linked, $[Ru_2(CO)_5(R\text{-}IAE)$ (3)], and a cluster product $[Ru_4(CO)_8(R\text{-}DAB)_2$ (4)], respectively. The reaction with R-DAB, yielding $Ru_2(CO)_5(R\text{-}IAE)$, proves that $Ru_2(CO)_5(R\text{-}DAB)$ is an intermediate in the earlier developed reaction of $Ru_2(CO)_6(R\text{-}DAB)$ with R-DAB.

Supplementary Material Available: Listings of elemental analyses data, anisotropic thermal parameters, bond lengths and bond angles, and observed and calculated structure factors (14 pages). Ordering information is given on any current masthead page.

Contribution from the Chemistry Department, Manchester University, Manchester M13 9PL, U.K., and Institut für Anorganische Chemie der Universität Göttingen, D-3400 Göttingen, West Germany

Preparation, Crystal Structure, and Spectroscopic Characterization of $[NEt_4]_2[Cu(SPh)_3]$

C. DAVID GARNER,*[1a] JOHN R. NICHOLSON,[1a] and WILLIAM CLEGG*[1b]

Received August 9, 1983

A new and convenient synthesis of $[Cu(SPh)_3]^{2-}$ involves the treatment of $[(Ph_3PCuCl)_4]$ with $[NEt_4]SPh$ (1:20) in MeCN. $[NEt_4]_2[Cu(SPh)_3]$ crystallizes in the monoclinic space group $P2_1/c$, with $a = 9.116$ (2) Å, $b = 13.107$ (2) Å, $c = 30.677$ (4) Å, $\beta = 95.39$ (1)°, $V = 3649$ Å^3, and $Z = 4$. The structure was solved by conventional Patterson and Fourier syntheses, and 4075 unique reflections were used in the refinement, which converged at $R = 0.074$. The copper(I) atom is coordinated by a trigonal-planar array of three sulfur atoms ($\overline{\text{Cu-S}} = 2.250$ (9) Å). IR, Raman, UV/visible, and ^{1}H NMR spectra are presented for this compound.

The preparation and crystal structure of $[PPh_4]_2[Cu(SPh)_3]$ have been reported by Coucouvanis et al.[2] This complex anion is of interest because, at present, it is the simplest fully characterized copper–thiolate complex and is thus valuable for the definition and interpretation of the spectroscopic properites typical of copper(I)–thiolate interactions. We were interested in this system, together with other copper(I)–thiolate clusters, particularly those prepared by Coucouvanis et al.[2,3] and Dance,[3] as possible models of the copper–cysteinyl aggregates suggested for metallothioneins, especially to aid interpretation of EXAFS data[4] for these proteins.

Investigations of the reactions of copper complexes with benzenethiolate have led to the following observations: (i) $[Cu(SPh)_3]^{2-}$ may be readily prepared in good yield by treating $[(Ph_3PCuCl)_4]$[5] with $[NEt_4]SPh$ (1:20), (ii) $[Cu(SPh)_3]^{2-}$ is intrinsically colorless *not* orange-red as previously observed in the $[PPh_4]^+$ salt,[2] and (iii) the Cu–S bond lengths for this anion, with $[NEt_4]^+$ as the cation, are more regular and, on average, slightly shorter than those reported[2] for the $[PPh_4]^+$ salt. These results, together with IR, Raman, UV/visible, and ^{1}H NMR spectra for $[NEt_4]_2[Cu(SPh)_3]$, are detailed herein.

Experimental Section

All manipulations were accomplished under an atmosphere of purified dinitrogen and the solvents used were purged with this gas. $[NEt_4]Cl$ (Fluka, 1.14 g, 6.88 mmol), dried by heating at ca. 100 °C in vacuo for ca. 4 h, was suspended in dry MeCN (normal commercial grade, ca. 7 cm^3). KSPh (1.02 g, 6.88 mmol) was added and the mixture stirred at room temperature for ca. 4 h. The precipitate thus obtained was removed by filtration, and to the resultant solution of $[NEt_4]SPh$ was added $[(Ph_3PCuCl)_4]$[5] (0.5 g, 0.34 mmol). The mixture was stirred at room temperature, and a clear solution was obtained after ca. 10 min, which was subsequently evaporated to dryness, under a reduced pressure and without heating. The off-white solid so obtained was washed three times with toluene (10-cm^3 portions) to remove Ph_3P and dried in vacuo. This solid was extracted into refluxing $i\text{-}Pr_2O$/MeCN (3 cm^3; 50:50 mixture by volume). Colorless needle-shaped crystals were obtained from this pale green/yellow solution upon slow cooling. These crystals were isolated by filtration, washed twice with a cold recrystallization medium, (ca. 2.0-cm^3 portions), and dried in vacuo; typical yield ca. 0.62 g (70%).

Anal. Calcd for $C_{34}H_{55}N_2CuS_3$: C, 62.7; H, 8.5; N, 4.3; Cu, 9.8; S, 14.8. Found: C, 62.5; H, 9.0; N, 4.5; Cu, 9.6; S, 14.4.

IR spectra were recorded on Perkin-Elmer 577 and 225 spectrometers, and Raman data were collected by using 514.5-nm excitation on a Spex double-monochromator Raman spectrometer. UV/visible absorptions were monitored ona Perkin-Elmer 402 spectrometer and the ^{1}H nuclear magnetic resonances observed at 300 MHz on a Varian SC-300 instrument.

Crystal Structure Determination

Crystals prepared as described above proved suitable for X-ray crystallographic studies. Measurements were made at room temperature on a Stoe-Siemens AED four-circle diffractometer, with graphite-monochromated Mo Kα radiation ($\lambda = 0.71069$ Å), from a crystal of dimensions 0.7 × 0.5 × 0.3 mm (parallelpiped with edges parallel to unit cell axes) sealed in a capillary tube. Cell dimensions were calculated by least-squares methods from the 2θ values ($20 < 2\theta < 25°$) of 52 centered reflections. The space group is $P2_1/c$ with $a = 9.116(2)$ Å, $b = 13.107$ (2) Å, $c = 30.677$ (4) Å, $\beta = 95.39$ (1)°, $V = 3649$ Å^3, $Z = 4$, and $D_{calcd} = 1.19$ g cm^{-3}.

Intensities were measured by a real-time profile-fitting method,[6] in a θ/ω scan mode for a unique set of reflections with $2\theta < 50°$; $h, k \geq 0$. Numerical absorption corrections were applied ($\mu = 7.87$ cm^{-1}, transmission 0.62–0.72). Of the 6390 unique data, 4075 with $F > 4\sigma(F)$ were used for the structure determination.[7] There was no significant variation in the intensities of three check reflections monitored regularly during the data collection.

The copper atom was located in a Patterson synthesis, and other atoms were located in subsequent difference maps. Hydrogen atoms were constrained [C–H = 0.96 Å, methyl H–C–H = 109.5°, aromatic H on C–C–C external bisector; $U(\text{H}) = 1.2U_{eq}(\text{C})$, where $U_{eq}(\text{C})$ is the equivalent isotropic thermal parameter for a C atom[8]]; all other atoms were refined with anisotropic thermal parameters, by a blocked

---

(1) (a) Manchester University. (b) Göttingen University.

(2) Coucouvanis, D.; Murphy, C. N.; Kanodia, S. K. *Inorg. Chem.* **1980**, *19*, 2993.

(3) Hollander, F. J.; Coucouvanis, D. *J. Am. Chem. Soc.* **1977**, *99*, 6268. McCandlish, L. E.; Bissell, E. C.; Coucouvanis, D.; Fackler, J. P.; Knox, K. *Ibid.* **1968**, *90*, 7357. Dance, I. G. *J. Chem. Soc., Chem. Commun.* **1976**, 68, 103. Dance, I. G.; Calabrese, J. C. *Inorg. Chim. Acta* **1976**, *19*, L41.

(4) Garner, C. D.; Hasnain, S. S.; Bremner, I.; Bordas, J. *J. Inorg. Biochem.* **1982**, *16*, 253; and work in progress. Bordas, J.; Koch, M. J. H.; Hartmann, H.-J.; Weser, U. *FEBS Lett.* **1982**, *140*, 19.

(5) Churchill, M. R.; Kalra, K. L. *Inorg. Chem.* **1974**, *13*, 1065.

(6) Clegg, W. *Acta Crystallogr., Sect. A* **1981**, *A37*, 22.

(7) All computer programs were written by G. M. Sheldrick (SHELXTL) and W. Clegg.

(8) Willis, B. T. M.; Pryor, A. W. "Thermal Vibrations in Crystallography"; University Press: Cambridge, U.K., 1975, p 101.